https://doi.org/10.5194/wcd-2020-19
Preprint. Discussion started: 27 May 2020

Weather and Climate Dynamics Discussions
Open Access
EGU

The role of heat flux-temperature covariance in the evolution of weather systems

Andrea Marcheggiani[1] and Maarten H.P. Ambaum[1]

[1]Department of Meteorology, University of Reading, Reading, UK

Correspondence: Andrea Marcheggiani (a.marcheggiani@pgr.reading.ac.uk)

Abstract. Local diabatic heating and temperature anomaly fields need to be positively correlated for the diabatic heating to produce work in the atmosphere. Here we quantify the thermodynamic contribution of local air–sea heat exchange on the evolution of weather systems using an index for the spatial covariance between heat flux at the air-sea interface and air temperature at 850 hPa upstream of the North Atlantic storm track, broadly corresponding with the Gulf Stream extension region. The index is found to be almost exclusively negative, indicating that the air–sea heat fluxes locally act as a sink on potential energy. It features bursts of high activity alternating with longer periods of lower activity. The characteristics of these high index bursts are studied through composite analysis and the mechanisms are investigated in a phase space spanned by two different index components. It is found that the negative peaks in the index correspond with thermodynamic activity triggered by the passage of a weather system over a spatially variable sea-surface temperature field; our results indicate that most of this thermodynamically active heat exchange is realised within the cold sector of the weather systems.

1 Introduction

In the Northern Hemisphere, storm tracks are longitudinally localised, with the main regions of intense storm track activity, both from an Eulerian (Blackmon et al., 1977) and a Lagrangian (Hoskins and Hodges, 2002) perspective, located off the eastern coasts of mid-latitude Asia and North America.

Hoskins and Valdes (1990) emphasise the local Eady growth rate, the *baroclinicity*, as the dynamically relevant variable to determine the geographical structure of the storm tracks. Ambaum and Novak (2014) point out the importance of baroclinicity in describing the temporal structure of storm tracks. They define a two-variable model which combines local baroclinicity and meridional eddy heat fluxes in a nonlinear oscillator and subsequently Novak et al. (2015) make use of it to explain regime transitions of the mid-latitude eddy-driven jet stream, which had been previously observed by Franzke et al. (2011). In particular, Novak et al. (2015) found that oscillations in baroclinicity and heat flux lead to variability in eddy anisotropy, which could then be associated with a major change in the dominant type of wave breaking (Hoskins et al., 1983), consequently affecting the jet stream latitudinal position, as is also observed in idealised experiments (Rivière, 2009; Orlanski, 2003).

Meridional heat fluxes can be interpreted as an indicator for the conversion of mean-flow to eddy available potential energy in the Lorenz energy cycle (Lorenz, 1955). Meridional and vertical heat fluxes act as conversion terms across different types of energy reservoirs, whereas surface heat fluxes are associated with generation of available potential energy.

https://doi.org/10.5194/wcd-2020-19
Preprint. Discussion started: 27 May 2020

Global estimates of these terms have been computed (Peixoto and Oort, 1992) and were used to identify the direction of energy flow within the Lorenz energy cycle. Novak et al. (2017) demonstrate that the dynamical relationship between storm track intensity and available potential energy as measured by baroclinicity can be described by a predator-prey relationship, whereby storm tracks can be thought of as *feeding* on baroclinicity.

The generation of eddy available potential energy can be described analytically by a term which is proportional to the covariance between surface heat flux and temperature (Lorenz, 1955; Peixoto and Oort, 1992; James, 1995). This term has been estimated to be positive globally (Oort, 1964; Oort and Peixoto, 1974; Ulbrich and Speth, 1991; Li et al., 2007; Marques et al., 2009), suggesting that diabatic processes are acting as a source of energy in storm development.

Diabatic processes at the surface, such as sensible and latent heat fluxes, amplify the horizontal temperature gradient by heating where it is warm and cooling where it is cold and thus generate available potential energy. From a global perspective this can be achieved by the global differential in radiative heating. However, the local thermodynamic effects of latent and sensible heat fluxes are much less clear: upward air–sea heat fluxes typically may be expected to coincide with a cooler local atmosphere, suggesting a negative contribution to the local potential energy budget.

The aim of this study is to identify and describe this local thermodynamic effect of air–sea heat fluxes. In this framework, heat flux–temperature spatial covariance is considered as a measure of the local contribution to diabatic generation or destruction of available potential energy and its evolution is linked to storm evolution.

This article is structured as follows: Section 2 briefly summarises the Lorenz energy cycle and the approach we take in our study. Section 3 introduces heat flux-temperature spatial covariance and examines its main features through the definition of an index. Section 4 investigates the driving mechanisms of the index previously introduced. Finally, in the final section results are summarised and discussed.

2 Lorenz Energy Cycle and flux–temperature covariance

Available potential energy can be generated globally through differential heating which amplifies meridional temperature gradients and gives the troposphere in the mid-latitudes a baroclinic structure favourable to the growth of extra-tropical weather systems (Peixoto and Oort, 1992). In the Lorenz energy cycle (Lorenz, 1955) the interaction between different types of energy reservoirs is represented by conversion terms while surface heat exchange appears in energy generation and dissipation terms. Global estimates of these terms have been computed (Oort, 1964; Oort and Peixoto, 1974; Ulbrich and Speth, 1991; Li et al., 2007; Marques et al., 2009) and they are found to differ not only in time from seasonal to inter-annual scales, but also depending on the type of data variability considered, be it purely temporal, spatial or a combinations of these. Oort (1964) found that generation of eddy available potential energy was negative in a spatial domain, whereas in a mixed space-time domain this was found to be positive. Ulbrich and Speth (1991) further decomposed eddy energy into stationary and transient components and estimated the former to be positive and the latter to be negative for January and July (averaged from 1980 to 1986) although with a difference in magnitude.

https://doi.org/10.5194/wcd-2020-19
Preprint. Discussion started: 27 May 2020

Weather and Climate Dynamics Discussions
Open Access
EGU

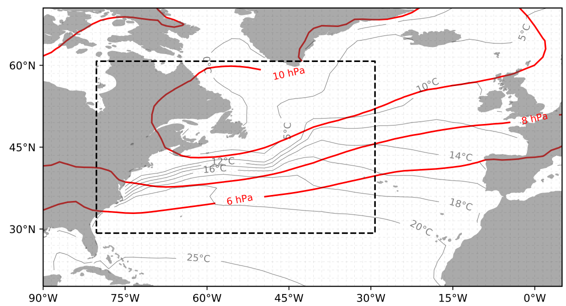

Figure 1. Wintertime SSTs climatology (black contours) and mean sea level pressure standard deviation in time (based on a 10-day running mean); the area within the dashed box (30–60°N, 30–79.5°W) corresponds to the region of the N. Atlantic considered in the next sections for the computation of spatial averages.

The generation terms have normally been estimated as residuals in the main balance equations, as data for their direct computation typically were not archived. Global estimates normally suggest a positive generation of eddy available potential energy, which would involve heating of warm and cooling of cold air masses. However, model experiments with simplified climate models, where diabatic heating is directly calculated, show a negative generation of eddy potential energy, with diabatic effects damping eddy available potential energy.

Given that storm tracks are by definition the main reservoirs of eddy potential energy, this begs the question of whether diabatic effects in storm tracks actually help or hinder their development, as investigated by Hoskins and Valdes (1990) who envisaged that sensible heating of cold air masses actually decreases the energy of weather systems while latent heating helps in their intensification in the warm sectors.

Here we take a hybrid approach: we use direct estimates of diabatic energy input over the upstream sector of the North Atlantic storm track region and use it to estimate whether it will serve as a source or as a sink of spatial variance in temperature. Available potential energy is a global weighted integral of such temperature variance. By defining a spatial covariance index between air–sea heat fluxes and lower atmospheric temperature we can quantify the extent to which the local heat fluxes help build available potential energy, or deplete it.

In particular, we consider the spatial covariance between time anomalies in instantaneous air–sea heat fluxes F' and air temperature T' at 850 hPa to define an area specific FT index,

$$\mathrm{FT} = \langle F'^{*} T'^{*} \rangle = \langle (F' - \langle F' \rangle)(T' - \langle T' \rangle) \rangle = \langle F'T' \rangle - \langle F' \rangle \langle T' \rangle, \tag{1}$$

where primes denote time anomalies with respect to a ten-day running mean, angle brackets spatial averages over the area selected and stars deviations from this spatial average.

https://doi.org/10.5194/wcd-2020-19
Preprint. Discussion started: 27 May 2020

Data come from the European Centre for Medium-Range Weather Forecast (ECMWF) Re-Analysis Interim dataset (ERA-Interim, (Dee et al., 2011)), restricting our attention to wintertime only (December to February, DJF), 6-hourly data from December 1979 to February 2019 (a total of 40 winters) interpolated onto a spatial grid with a resolution of 1.5° in both latitude and longitude. In order to concentrate on synoptic scale variability, time anomalies are defined as deviations from a running mean with a time window of 10 days (Athanasiadis and Ambaum, 2009). Instantaneous surface sensible heat fluxes have been utilised as a measure for heat exchange, F, which is defined as positive if heat flows upwards from the ocean to the atmosphere.

Repeating our analysis with latent heat fluxes or the sum of latent and sensible heat fluxes did not change the outcomes, although values depending on heat flux magnitude of course change. The fact that the analysis seems mostly independent of which flux is used indicates that the space and time filtered fluxes have a broadly fixed Bowen ratio.

The FT index was calculated over the western North Atlantic, extending between $30-60°$N and $30-79.5°$W. The domain selected is shown in Fig. 1, together with sea surface temperatures (SSTs) wintertime climatology and the time standard deviation of mean sea level pressure. The domain selected coincides with both the upstream region of the storm track (region of stronger mean sea level pressure time variance) and the Gulf Stream extension (strongest SST gradient), where the largest SST variability is observed across different scales (e.g. large-scale meridional gradients and small-scale oceanic eddies). Additionally, in the computation of the FT index land grid points are masked out in order to concentrate on air–sea interaction only.

3 Temporal properties of the FT index

Figure 2 (top) shows the temporal behaviour of the FT index, Eq. 1, as defined for the upstream region of the North Atlantic storm track.

The index is found to be always negative and it features moderately frequent (strongest 5th percentile occurring once every 2–3 weeks) bursts of intense activity peaking at values down to almost $-1500\ \mathrm{W\,m^{-2}\,K}$ among periods of weaker activity during which the index fluctuates around values closer to zero, still keeping its negative sign. This reflects on the empirical distribution of the index values, plotted to the right of the index time series in Fig. 2, featuring large skewness and an extended tail towards negative values.

The empirical distributions for the local values of F'^{*}, T'^{*} and $F'^{*}T'^{*}$ are shown in Fig. 2 (bottom left to right respectively). More than 9.5×10^{6} data points across both the spatial and time domain were used, which allowed for the distributions in Fig. 2 to result sufficiently smooth to be examined without any sort of data filtering. These anomalies correspond to the anomalous fields constructed in order to calculate the index, which is the spatial average of $F'^{*}T'^{*}$. The distribution for heat flux space-time anomalies is distinctively skewed towards negative values, whereas temperature anomalies follow more a Gaussian distribution. This is consistent with the different heat capacities of the atmosphere and the ocean, as the atmosphere is more easily heated by the ocean, while it takes both a longer time and a stronger vertical gradient in temperature for the atmosphere to flux heat into the ocean.

https://doi.org/10.5194/wcd-2020-19
Preprint. Discussion started: 27 May 2020

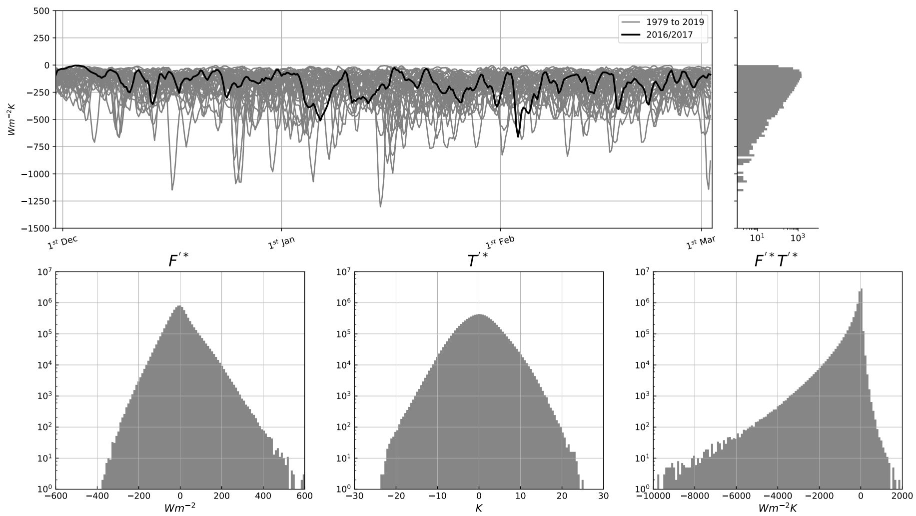

Figure 2. Top: Index time series computed over the upstream region of the N. Atlantic storm track (30–60°N, 30–79.5°W), spanning the full ERA-Interim time series (grey solid lines), highlighting a sample season (2016/2017 winter, solid black line); (right) empirical distribution of index values (semi-log scale). Bottom: Empirical distribution of instantaneous space-time anomalies in surface heat flux and temperature over the upstream region (semi-log scale).

The sporadic nature of the strong negative index values suggest a link with weather system activity, as observed in for example in Messori and Czaja (2013a) and Ambaum and Novak (2014). Evidence for this link is shown in Fig. 3, where composites on the strongest and weakest FT index values are shown for mean sea level pressure, air temperature at 850 hPa and surface sensible heat flux. Strong FT index values (in the most negative 5th percentile) correspond to patterns associated with a low pressure system, with stronger than usual surface heat flux coinciding with cold air being advected from the American continent. Weak FT index (values in the top 5th percentile) correspond instead to inhibited storm activity, with weaker surface heat flux consistent with a pressure pattern which leads to weakened low level westerlies.

Lagged composites centred on extreme events were computed (not shown) for mean sea level pressure, air temperature and precipitation rates, both convective and large-scale (as available from ERA Interim, Dee et al. 2011). Between four and three days before the peak intensity in the FT index is reached, a low pressure system was observed entering the spatial domain, then intensifying at the FT index peak and finally decaying within synoptic time scales (three–four days).

Arguably, the intensification and decay phases observed in lagged composites could be deriving from a gain/loss of signal due to averaging of several different kinds of events, especially at longer lags. However, the decay phase was observed to be relatively rapid compared to the intensification phase, as weather patterns leading to the peak were observed to last longer than those in the decay phase. This asymmetry between the initial and final stages of the FT index intensification is consistent with the idea that a strong negative FT index indicates thermodynamic sink on the system.

https://doi.org/10.5194/wcd-2020-19
Preprint. Discussion started: 27 May 2020

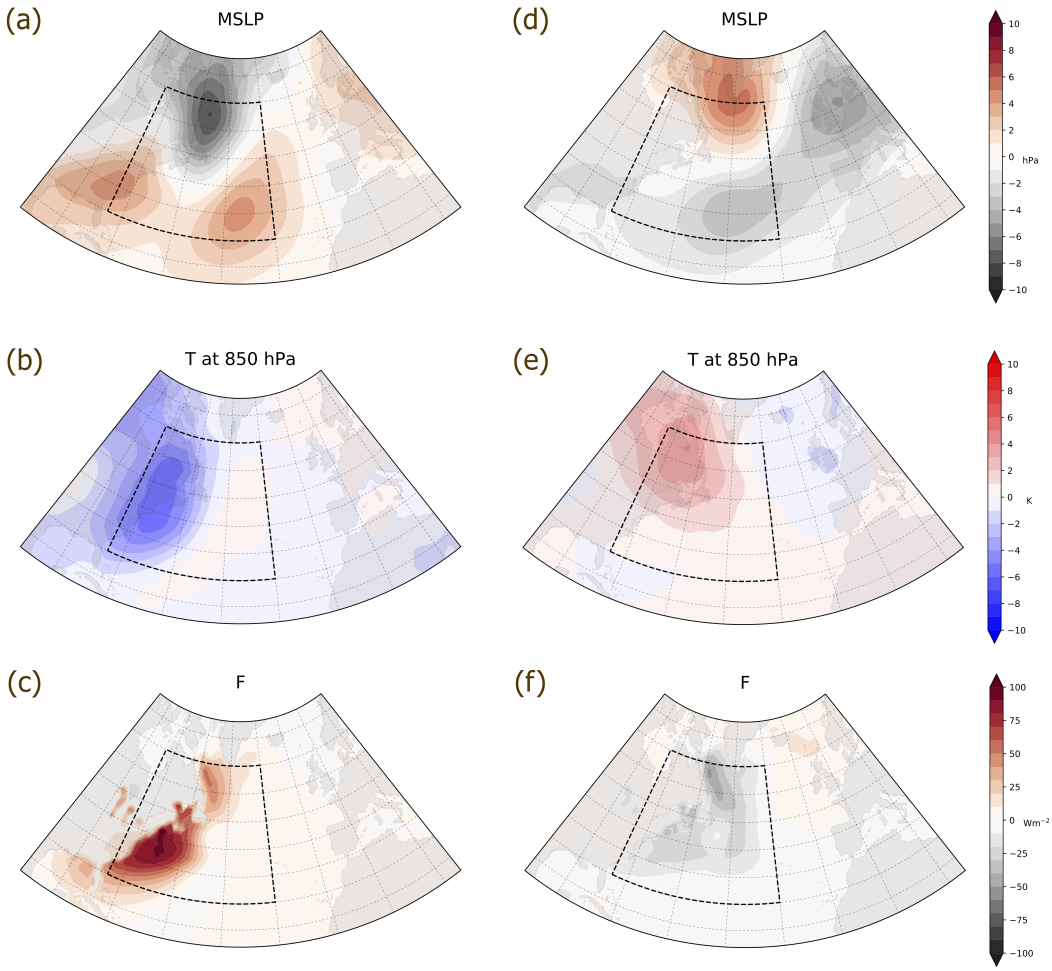

Figure 3. Composites on strongest (a–c) and weakest (d–f) FT index values (top and bottom 5th percentiles) for mean sea level pressure (a,d), air temperature at 850 hPa (b,e) and surface sensible heat flux (c,f). Colour shadings represent difference between composites and winter climatology; dashed boxes indicate the spatial domain where the FT index is defined.

Surface heat flux and temperature distributions are almost symmetric, centred on values relatively close to zero compared to extreme events in the tails, and feature weak skewness. The product of these anomalies, on the other hand, shows an asymmetric distribution markedly skewed towards negative values with a long negative tail, indicating strong local negative correlation between the two variables.

The FT index is the spatial average of this signal and it is never positive. Any positive index would correspond to heat flowing from an anomalously cold sea-surface to an anomalously warm air mass (and vice versa) which is less likely given that the air–sea heat fluxes are parameterised in terms of the temperature difference between the sea surface and the lower atmosphere.

However, high instability in the lowest layers of the troposphere could cause the index to become positive, as air temperature at 850 hPa is not directly used in the computation of surface heat fluxes. Furthermore, the transfer coefficient is a non-trivial function of boundary layer properties, not directly linked to the temperature at 850 hPa. It is therefore a non-trivial result that the FT index is observed to be negative at all times.

Note in addition that the FT index is primarily a measure of spatial variability and concurrent positive (negative) anomalies in flux and temperature do not necessarily correspond to stronger (weaker) values compared to climatology, but would indicate stronger (weaker) intensity compared to both the surrounding area and the previous and following 5 days. We also found weaker negative index values to be indicative primarily of diminished storm activity, as Fig. 3 shows. Hence, it seems reasonable to interpret any positive instances as indicative of a relatively weak heat exchange.

4 Phase-space properties of the FT index

We expect the FT index to be associated with variations in storm track properties. In order to get a clear picture of these associations we will employ a phase space kernel averaging technique.

The phase space is spanned by two variables. Any quantity can be kernel-averaged at any point in the phase space. We thus obtain a picture of how the quantity will depend on the two variables spanning the phase space.

A particularly interesting quantity to represent in such phase space is the tendency of the variables that span the phases space. In this way we can construct a flow in the phase space, representing the kernel averaged tendencies in the data.

The technical details of constructing the phase space averages and tendencies are described in (Novak et al., 2017)). They constructed a two-dimensional phase space where they were able to identify a predator-prey relationship between meridional heat fluxes and mean baroclinicity respectively, as these were used as coordinates in the phase space. Results may vary somewhat according to kernel size chosen, though in our study the results were observed to be broadly independent of the size of the kernel used (not shown).

We start our analysis by constructing a phase space spanned by the FT index and mean baroclinicity in our chosen N. Atlantic storm track domain. The kernel averaged phase tendencies for the FT index and mean baroclinicity are shown in Fig. 4.

We find that the circulation in the FT–baroclinicity phase space lies almost entirely on the negative side of the FT index axis and it is in the anti-clockwise direction. Furthermore, it can be observed that mean baroclinicity is depleted when the FT index is strengthening and it recovers only at lower FT index values. This is consistent with results of composite analysis, as baroclinicity was found to be depleted during extreme events in the FT index.

This suggests that the flux-temperature spatial covariance plays an important role in the budget for mean baroclinicity (and available potential energy, more generally) and any mechanism driving the FT index should be linked to storm evolution.

In fact, this result suggest that the FT index is a good measure of processes that deplete baroclinicity.

The FT index can be decomposed into the product of flux-temperature spatial correlation and spatial standard deviations in flux and temperature,

$$\text{FT index} = \text{cov}(F', T') \equiv \text{corr}(F', T')\,\sigma(F')\,\sigma(T'). \tag{2}$$

https://doi.org/10.5194/wcd-2020-19
Preprint. Discussion started: 27 May 2020

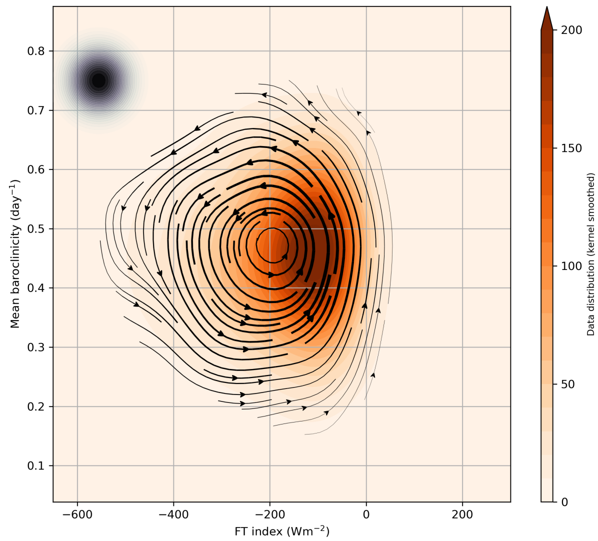

Figure 4. Kernel-averaged circulation in the FT index-mean baroclinicity phase space. Streamlines correspond to kernel-averaged rates of change in FT and baroclinicity (line thickness proportional to phase speed, plotted where data density is larger than 10). Shading represents kernel-smoothed data density.

This suggests we can also use spatial standard deviations in F and T as coordinates of the phase space where trajectories traced by the index components would represent its evolution across the various components of the index.

The occurrence of strong index values can be explained by increasing variance in either heat flux or temperature, or anomalously strong correlations between the two variables. Another possibility is of course that a combination of any of these three factors produces strong index events.

This question of magnitude driven or phase driven index extremes is similar to that presented in Messori and Czaja (2013b) for meridional heat transport although we use a different approach to determine which case is closest to reality through phase tendencies analysis.

Figure 5a shows the picture resulting from kernel-averaging in our phase space spanned by the variances in heat flux and air temperature. Here streamlines indicate the phase space mean trajectories and their thickness is proportional to the phase speed, while the shading represents the typical value of the FT index at each point in the phase space as resulting from kernel-averaging, i.e. its phase tendency.

Regions in the phase space where data is scarce (less than 10 and 1 data points respectively for streamlines and phase tendencies) are hidden as kernel-averages there are not representative of the local value of the variable.

https://doi.org/10.5194/wcd-2020-19
Preprint. Discussion started: 27 May 2020

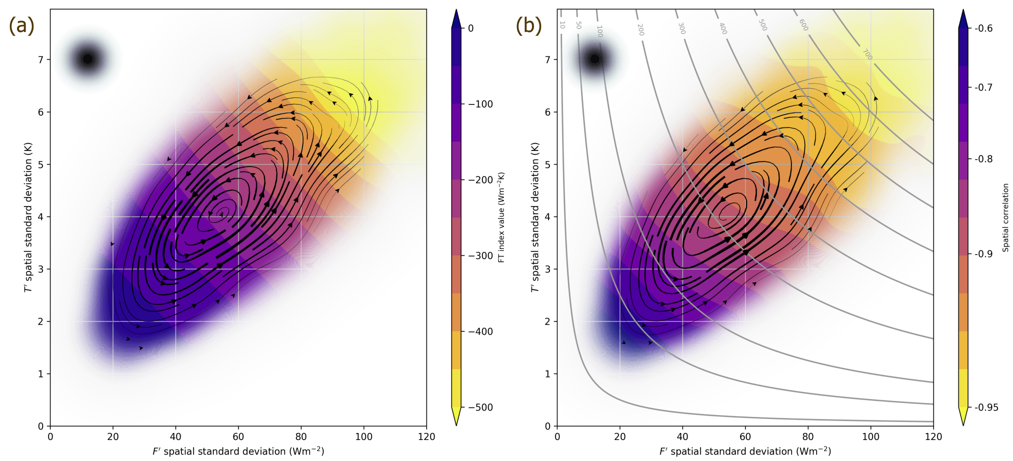

Figure 5. Kernel-averaged circulation in the F'-T' spatial standard deviations phase space. Streamlines correspond with kernel-averaged trajectories traced by the product of spatial standard deviations (line thickness proportional to phase speed, plotted where data density is larger than 10). Shading represent phase tendencies for the FT index and FT spatial correlation in panels (a) and (b) respectively. Grey contours in panel (b), drawn at 10 Wm^{-2}K, 50 Wm^{-2}K, 100 Wm^{-2}K and then every 100 Wm^{-2}K, indicate the product of spatial standard deviations.

The trajectories traced by the FT index components are found, on average, to be oscillating between low and high values of the index, which is consistent with the behaviour observed in the time series and shows that stronger index values are associated with larger variances in F' and T'.

The trajectories are also observed to be oscillating between weak and strong F'-T' spatial correlation, as shown by spatial correlation phase tendencies illustrated in Fig. 5b.

Taking a closer look at the relationship between spatial correlation and standard deviations in F' and T', these appear to be growing concurrently. This can be deduced by inspecting Fig. 5b, as spatial correlation is observed to increase together with the product of spatial standard deviations in F' and T', which is represented by grey contours.

In Fig. 6, spatial correlation is plotted against the product of standard deviations in F' and T' using values from the phase tendency in Fig. 5b (dark-grey dots) and then compared with raw data (light-grey dots) in order to exclude it being an artefact of kernel-averaging. Spatial correlation and variances are found to be in an almost log-linear relationship, with phase tendencies indicating increases in correlation as strongly linked to increases in variances, while raw data point perhaps to an even stronger link.

These results suggest that the observed bursts in flux-temperature spatial covariance are neither exclusively phase-driven nor exclusively magnitude-driven. Both high flux and air temperature spatial variability and correlation are characteristic features

https://doi.org/10.5194/wcd-2020-19
Preprint. Discussion started: 27 May 2020

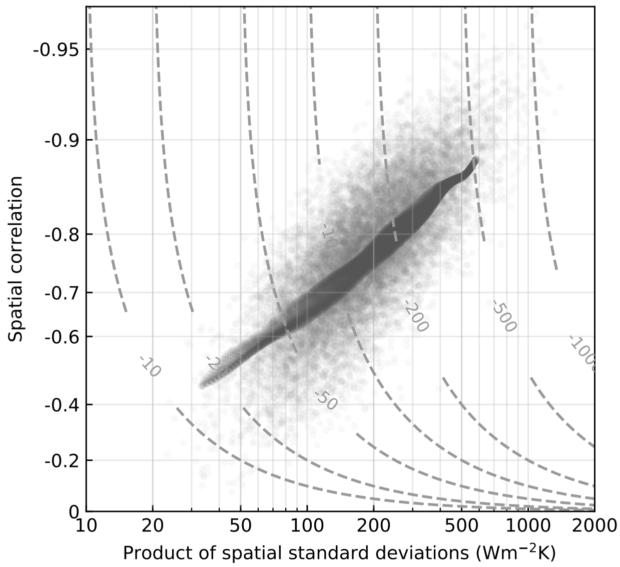

Figure 6. Scatter plot of F'-T' spatial correlation against the product of F' and T' standard deviations using kernel-averaged data points from phase portrait (dark shading) and raw data (grey dots); grey contours ($Wm^{-2}K$) indicate FT index value.

of the bursts. We conclude that both strength and correlation in spatial variability are equally fundamental to the build up of flux-temperature spatial covariance.

It is not clear why the correlation between the two variables increases so markedly with their variability. The simple model of flux being essentially proportional to the temperature at 850 hPa would not exhibit such a behaviour.

The simultaneous growth of correlation and variance is a non-trivial result and it suggests further research into assessing whether this is a general feature of the relationship between flux and lower atmospheric temperature or if it is limited to spatial variability dynamics or to the specific timescales considered. This would go beyond the scope of the present paper, but preliminary analysis indicates that the increase of correlation with variance may be a more generic property of the relationship between air–sea flux and lower atmosphere temperature.

The kernel-averaged trajectories in the phase space are organised in concentric ellipses, which suggests that the evolution of the FT index is cyclical in nature. By computing the average phase speed at which the trajectories are traced, it is estimated that it takes between 4 and 6 days for the FT index to go round a full cycle (see Fig. 8a for a sample trajectory). This time frame (4-6 days) falls within the range of synoptic timescales, consistently with the idea that the index is closely linked to the evolution of a storm system.

We then notice that the observed circulation spins in an anticlockwise direction. This indicates that the spatial variability in F' leads the spatial variability in T', as can be seen by following any of the trajectories starting from weak index values.

https://doi.org/10.5194/wcd-2020-19
Preprint. Discussion started: 27 May 2020

Weather and Climate Dynamics Discussions
Open Access
EGU

This may be somewhat counter-intuitive, but can be explained by the advection of the cold air mass, in the cold sector of a weather system, moving over a more spatially variable SST field such as that of the Gulf Stream extension. SST variability would trigger heat flux spatial variance which would then lead to temperature variance generation.

The idea of the cold sector playing a primary role in the evolution of the FT index is further supported by the study of phase tendencies in F and T.

Figure 7 shows phase tendencies for spatial-mean heat flux F and air temperature T. We find that the growing phase of the FT index coincides with a decrease in mean T and a concomitant increase in mean F. A decay phase then follows, characterised by the opposite trends.

Heat flux anomalies range from -20 Wm^{-2} in the decay phase up to 40 Wm^{-2} in the growing phase, while air temperature anomalies stretch between -2 K and 2 K respectively. The standard deviations in time of spatial-mean F and T are respectively 23.3 Wm^{-2} and 2.2 K, suggesting that these signals do not arise exclusively from random fluctuations and thus providing our results with robustness.

Phase tendencies in Fig. 7 may be explained by relating the growing and decaying phases to an increased dominance of the cold sector of weather systems in the former, while the warm sector influences the latter. This would be in agreement with composite analyses for convective precipitation (not shown), which showed a precipitation band coinciding with the cold front as identifiable from the air temperature composite.

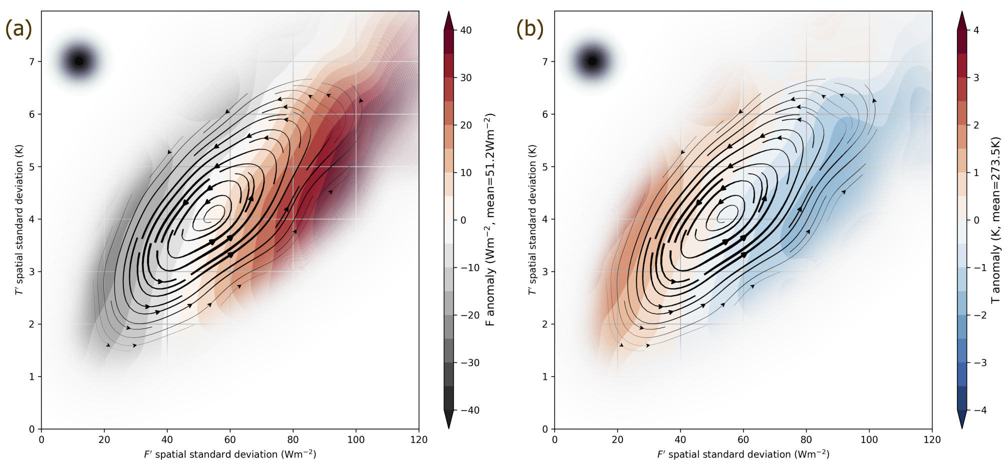

Figure 7. Phase tendencies for spatial-mean F (a) and T (b). Shading represent difference between phase tendency and the mean value of F and T, as reported next to each colour bar. Streamlines as in Fig. 5.

Further evidence to the importance of cold and warm sectors in the evolution of the FT index is found as follows. A closed trajectory in phase space is chosen by selecting a line of constant value of the stream function which was computed to draw the streamlines shown in the phase portraits. The selected closed trajectory crosses regions of high data density so that it corresponds to a larger number of unfiltered trajectories (i.e. not kernel-averaged) thus more likely to be representative of real events rather than just of a mean behaviour.

Figure 8b shows the difference between the kernel-averaged potential temperature vertical profiles and climatology along the closed phase space trajectory shown in Fig. 8a, which takes around 5 days to complete. The kernel-averaged mean boundary layer height is also shown by a black solid line. The cold and warm phases are characterised respectively by deeper and shallower atmospheric boundary layer. This is consistent with the idea that growing phase corresponds to the advection of the cold sector into the spatial domain over a warmer SST leading to instability and convective heat fluxes.

A downward propagation of the temperature anomalies is also observed, especially in the cooling phase where the temperature anomalies are largest, as the cold sector moves across the spatial domain. The strongest anomalies are observed in the lower layers of the troposphere, which is symptomatic of the close relationship between the FT index and surface heat exchange, as per definition of the index itself.

The warm phase coincides with a shallower boundary layer, as warm air is advected over the cold side of the SST front, which results in a more stable atmospheric boundary layer and weaker heat exchange. Indeed, the sea surface does not reach temperatures as low as in the preceding cold sector, hence it does not interact as strongly as in the cold phase and this could explain the rapid decay of the heat flux–temperature spatial covariance.

These results are not sensitive to the choice of the specific closed phase space trajectory (not shown).

The heat exchange within a cold sector arguably plays a primary role in driving the FT index. The phase tendency of the area fraction of the spatial domain occupied by the cold sector, shown in Fig. 9, illustrates this further. To estimate the area fraction, we utilise a a diagnostic based upon potential vorticity at the 95kPa level as proposed in a study by Vannière et al. (2016), where it is shown that the cold sector is characterised by a negative potential vorticity signature which proved to be effective as a diagnostic through the comparison with more traditional indicators of the cold sector of extra-tropical weather systems.

In the strengthening phase of the FT index life cycle, the extent of the cold sector almost doubles from about 20% to almost 40% of the domain. This suggests that air–sea heat exchange in the cold sector has significant effects on storm evolution, in particular by driving the depletion of the baroclinicity over the domain. This appears to be in contradiction with earlier findings in Vannière et al. (2017), where it was suggested that baroclinicity is mainly restored in the cold sector.

Looking at specific events in the FT index, we find that surface heat flux and SST fields are well correlated, especially over warmer sea surfaces. SSTs over the Gulf Stream extension region are indeed characterised by higher spatial variability than air temperatures due to the presence of mesoscale oceanic eddies in the Gulf Stream.

Oceanic mesoscale eddies have been shown to play a decisive role in shaping the North Atlantic storm track as they support stronger storm growth rates, making their representation essential for a better description of the storm track (Ma et al., 2017; Zhang et al., 2019). In particular, Foussard et al. (2019) examined the effect of oceanic eddies on storm tracks through an idealised experiment focused on the mid-latitudes, observing a poleward shift of storm trajectories compared to simulations in which mesoscale eddies are removed, as found by Ma et al. (2017) in more realistic simulations for the North Pacific. Foussard et al. (2019) noticed also a larger sensitivity of the atmosphere to positive than to negative anomalies in SST, as the former correspond to a stronger temperature gradient at the air–sea interface.

https://doi.org/10.5194/wcd-2020-19
Preprint. Discussion started: 27 May 2020

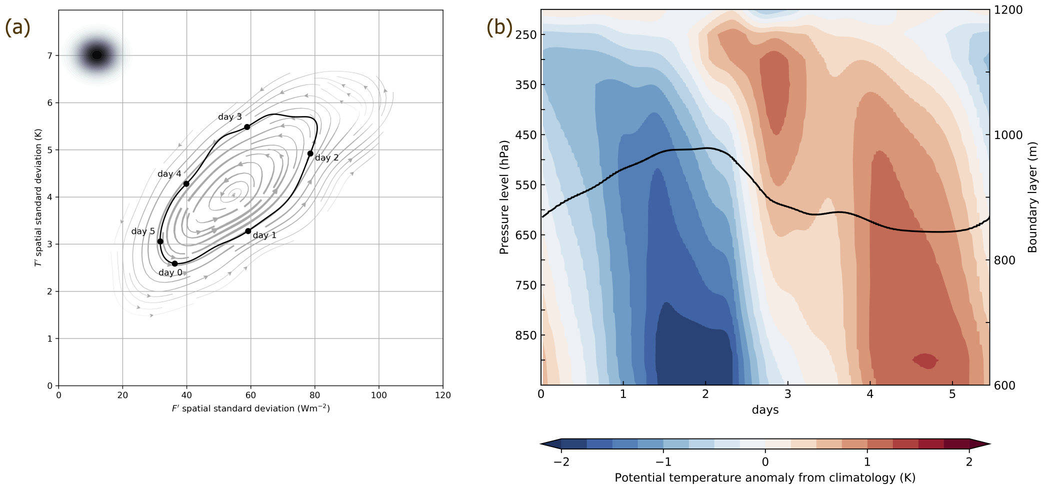

Figure 8. Phase tendency analysis (b) for area-averaged potential temperature profile (colour shading, difference from winter climatology) and boundary layer height (dashed line) along the closed trajectory shown in panel (a). The horizontal coordinate axis indicates the time progression along the closed trajectory in days.

In light of this, we can conclude that in the FT index growing phase the trigger for heat flux variability corresponds to the advection of (relatively) uniformly cold air masses over the spatially varying SSTs of the Gulf Stream extension region. The strong vertical contrast in temperatures causes enhanced surface heat fluxes which then lead to a reaction in the lower atmosphere which experiences a subsequent increase in temperature spatial variability.

5 Conclusions

Lorenz (1955) showed that diabatic generation of available potential energy is proportional to the covariance between heating and air temperature. This term has been estimated to be positive as the residual of momentum and thermodynamic equations and therefore assumed to act as a source of energy for weather systems to feed on. However, using data for surface heat fluxes and air temperatures from ERA-Interim, we find that they are locally negatively correlated in time and space, in particular upstream of the N. Atlantic storm track.

We investigate the heat flux–temperature covariance through the definition of an index (FT index) that measures the local spatial covariance between sensible heat flux and air temperature at 850 hPa. To that effect, a hybrid approach was taken where anomalies are defined as deviations from a spatial mean relative to a limited spatial domain, in our case, the Gulf Stream extension region.

The FT index is found to be always negative and characterised by bursts of activity coinciding with strong synoptic storm activity within the spatial domain considered. Composite analysis of strong index values suggest that heat flux-temperature

https://doi.org/10.5194/wcd-2020-19
Preprint. Discussion started: 27 May 2020

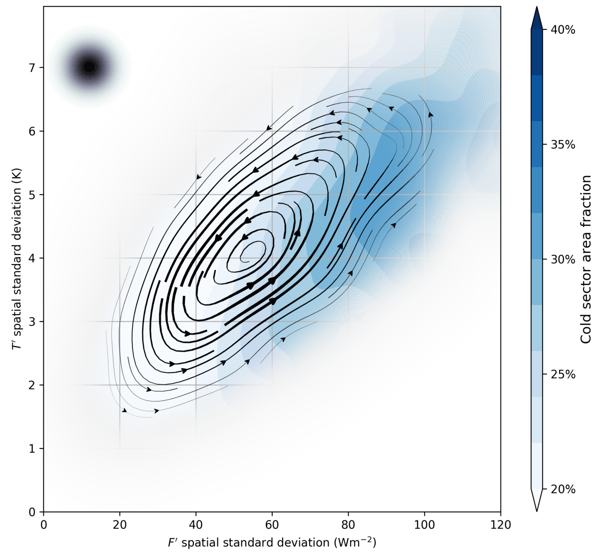

Figure 9. As in Fig. 7, for the phase tendency of cold sector area fraction (percentage of spatial domain occupied by cold sector).

spatial covariance behaves as an energy sink in the evolution of a storm. The peak of the FT index coincides with the start of the decaying phase of the storm. This is in contrast with global estimates obtained for the Lorenz energy cycle.

Heat flux-temperature spatial covariance, as measured by the FT index, and available potential energy, as identified by baroclinicity, are seen to be interacting in a cyclical evolution. Strong FT index values coincide with baroclinicity depletion, while only with a weaker FT index baroclinicity is seen to recover.

Spatial correlation and standard deviations in heat fluxes and air temperatures are observed to be equally important in the build up of strong spatial covariance, with an increase of spatial variability in surface heat fluxes typically preceding an increase for air temperatures spatial variability.

In fact we find, rather counter-intuitively, that the correlation between flux and temperature increases strongly with their variances.

The intensification phase of the FT index coincides with the passage of a storm's cold sector across the region considered. The advection of cold air masses across the meridional sea surface temperature gradient and mesoscale oceanic eddies then leads to an increased spatial variability in the surface heat flux field, which eventually bring the FT index to peak values, as heat flux and temperature fields correlate spatially.

https://doi.org/10.5194/wcd-2020-19
Preprint. Discussion started: 27 May 2020

Data availability. In this study we utilised ECMWF ERA-Interim data, which can be downloaded from the ECMWF web page at https://apps.ecmwf.int/datasets/.

Author contributions. AM performed data analyses and prepared the manuscript. MHPA originated the idea for the study, contributed to the interpretation of the results and improved the manuscript.

Competing interests. The authors declare that they have no conflict of interest.

Acknowledgements. AM acknowledges PhD studentship funding from the Scenario NERC Doctoral Training Partnership grant NE/R008868/1, co-sponsored by the UK Met Office. The authors thank ECMWF for their ERA-Interim Reanalysis data.

References

Ambaum, M. H. and Novak, L.: A nonlinear oscillator describing storm track variability, Quarterly Journal of the Royal Meteorological Society, 140, 2680–2684, 2014.

Athanasiadis, P. J. and Ambaum, M. H. P.: Linear Contributions of Different Time Scales to Teleconnectivity, Journal of Climate, 22, 3720–3728, https://doi.org/10.1175/2009JCLI2707.1, https://doi.org/10.1175/2009JCLI2707.1, 2009.

Blackmon, M. L., Wallace, J. M., Lau, N.-C., and Mullen, S. L.: An observational study of the Northern Hemisphere wintertime circulation, Journal of the Atmospheric Sciences, 34, 1040–1053, 1977.

Dee, D. P., Uppala, S., Simmons, A., Berrisford, P., Poli, P., Kobayashi, S., Andrae, U., Balmaseda, M., Balsamo, G., Bauer, d. P., et al.: The ERA-Interim reanalysis: Configuration and performance of the data assimilation system, Quarterly Journal of the royal meteorological society, 137, 553–597, 2011.

Foussard, A., Lapeyre, G., and Plougonven, R.: Storm track response to oceanic eddies in idealized atmospheric simulations, Journal of Climate, 32, 445–463, 2019.

Franzke, C., Woollings, T., and Martius, O.: Persistent circulation regimes and preferred regime transitions in the North Atlantic, Journal of the atmospheric sciences, 68, 2809–2825, 2011.

Hoskins, B. and Hodges, K.: New perspectives on the Northern Hemisphere winter storm tracks, Journal of the Atmospheric Sciences, 59, 1041–1061, 2002.

Hoskins, B. J. and Valdes, P. J.: On the existence of storm-tracks, Journal of the atmospheric sciences, 47, 1854–1864, 1990.

Hoskins, B. J., James, I. N., and White, G. H.: The shape, propagation and mean-flow interaction of large-scale weather systems, Journal of the atmospheric sciences, 40, 1595–1612, 1983.

James, I. N.: Introduction to circulating atmospheres, Cambridge University Press, 1995.

Li, L., Ingersoll, A. P., Jiang, X., Feldman, D., and Yung, Y. L.: Lorenz energy cycle of the global atmosphere based on reanalysis datasets, Geophysical Research Letters, 34, 2007.

Lorenz, E. N.: Available potential energy and the maintenance of the general circulation, Tellus, 7, 157–167, 1955.

Ma, X., Chang, P., Saravanan, R., Montuoro, R., Nakamura, H., Wu, D., Lin, X., and Wu, L.: Importance of resolving Kuroshio front and eddy influence in simulating the North Pacific storm track, Journal of Climate, 30, 1861–1880, 2017.

Marques, C. A., Rocha, A., Corte-Real, J., Castanheira, J. M., Ferreira, J., and Melo-Gonçalves, P.: Global atmospheric energetics from NCEP–Reanalysis 2 and ECMWF–ERA40 Reanalysis, International Journal of Climatology: A Journal of the Royal Meteorological Society, 29, 159–174, 2009.

Messori, G. and Czaja, A.: On the sporadic nature of meridional heat transport by transient eddies, Quarterly Journal of the Royal Meteorological Society, 139, 999–1008, https://doi.org/10.1002/qj.2011, https://rmets.onlinelibrary.wiley.com/doi/abs/10.1002/qj.2011, 2013a.

Messori, G. and Czaja, A.: On the sporadic nature of meridional heat transport by transient eddies, Quarterly Journal of the Royal Meteorological Society, 139, 999–1008, 2013b.

Novak, L., Ambaum, M. H., and Tailleux, R.: The life cycle of the North Atlantic storm track, Journal of the Atmospheric Sciences, 72, 821–833, 2015.

Novak, L., Ambaum, M., and Tailleux, R.: Marginal stability and predator–prey behaviour within storm tracks, Quarterly Journal of the Royal Meteorological Society, 143, 1421–1433, 2017.

Oort, A. H.: On estimates of the atmospheric energy cycle, Mo. Wea. Rev, 92, 1964.

https://doi.org/10.5194/wcd-2020-19
Preprint. Discussion started: 27 May 2020

Oort, A. H. and Peixoto, J. P.: The annual cycle of the energetics of the atmosphere on a planetary scale, Journal of Geophysical Research, 79, 2705–2719, 1974.

Orlanski, I.: Bifurcation in eddy life cycles: Implications for storm track variability, Journal of the atmospheric sciences, 60, 993–1023, 2003.

Peixoto, J. P. and Oort, A. H.: Physics of climate, New York, NY (United States); American Institute of Physics, 1992.

Rivière, G.: Effect of latitudinal variations in low-level baroclinicity on eddy life cycles and upper-tropospheric wave-breaking processes, Journal of the Atmospheric Sciences, 66, 1569–1592, 2009.

Ulbrich, U. and Speth, P.: The global energy cycle of stationary and transient atmospheric waves: results from ECMWF analyses, Meteorology and Atmospheric Physics, 45, 125–138, 1991.

Vannière, B., Czaja, A., Dacre, H., Woollings, T., and Parfitt, R.: A potential vorticity signature for the cold sector of winter extratropical cyclones, Quarterly Journal of the Royal Meteorological Society, 142, 432–442, 2016.

Vannière, B., Czaja, A., and Dacre, H. F.: Contribution of the cold sector of extratropical cyclones to mean state features over the Gulf Stream in winter, Quarterly Journal of the Royal Meteorological Society, 143, 1990–2000, 2017.

Zhang, X., Ma, X., and Wu, L.: Effect of Mesoscale Oceanic Eddies on Extratropical Cyclogenesis: a Tracking Approach, Journal of Geophysical Research: Atmospheres, 2019.